ARMY RESEARCH LABORATORY

Electromagnetic Wave Scattering from Particles of Arbitrary Shapes

by Dmitry Petrov, YuriyShkuratov, and GordenVideen

ARL-RP-0443 **June 2013**

This is a reprint from the *Journal of Quantitative Spectroscopy & Radiative Transfer*, 112, (2011), 1636–1645.

Approved for public release; distribution unlimited.

NOTICES

Disclaimers

Army Research Laboratory

Adelphi, MD 20783-1197

ARL-RP-0443 **June 2013**

Electromagnetic Wave Scattering from Particles of Arbitrary Shapes

Dmitry Petrov and YuriyShkuratov
Astronomical Institute of Kharkov
V. N. Karazin National University,
35 Sumskaya St, Kharkov 61022, Ukraine

GordenVideen
Computational and Information Sciences Directorate, ARL

This is a reprint from the *Journal of Quantitative Spectroscopy & Radiative Transfer*, 112, (2011), 1636–1645.

REPORT DOCUMENTATION PAGE

Form Approved
OMB No. 0704-0188

1. REPORT DATE *(DD-MM-YYYY)*	2. REPORT TYPE	3. DATES COVERED (From - To)
June 2013	Reprint	

4. TITLE AND SUBTITLE
Electromagnetic Wave Scattering from Particles of Arbitrary Shapes

5a. CONTRACT NUMBER

5b. GRANT NUMBER

5c. PROGRAM ELEMENT NUMBER

6. AUTHOR(S)
Dmitry Petrov, YuriyShkuratov, and GordenVideen

5d. PROJECT NUMBER

5e. TASK NUMBER

5f. WORK UNIT NUMBER

7. PERFORMING ORGANIZATION NAME(S) AND ADDRESS(ES)
U.S. Army Research Laboratory
ATTN: RDRL-CIE-S
2800 Powder Mill Road
Adelphi, MD 20783-1197

8. PERFORMING ORGANIZATION REPORT NUMBER
ARL-RP-0443

9. SPONSORING/MONITORING AGENCY NAME(S) AND ADDRESS(ES)

10. SPONSOR/MONITOR'S ACRONYM(S)

11. SPONSOR/MONITOR'S REPORT NUMBER(S)

12. DISTRIBUTION/AVAILABILITY STATEMENT
Approved for public release; distribution unlimited.

13. SUPPLEMENTARY NOTES
This is a reprint from the *Journal of Quantitative Spectroscopy & Radiative Transfer*, 112, (2011), 1636–1645.

14. ABSTRACT
We consider a general solution of the electromagnetic wave scattering problem for arbitrarily shaped homogeneous particles, whose surface can be expressed by a function of angular coordinates, using a Laplace series expansion. This can include regularly shaped particles (e.g., ellipsoids and cubes) as well as irregularly shaped particles like Gaussian spheres. For calculations of scattering properties of the particles, we use the approach based on the *Sh*-matrix. The *Sh*-matrix elements deduced from the *T*-matrix technique allow one to separate the shape effects from size- and refractive-index-dependent parameters. The separation also allows the corresponding surface integrals to be solved analytically for different particle shapes. In this manuscript, we give analytical expressions for the *Sh*-matrix elements for arbitrary shaped particles that can be presented with Laplace series. We find good agreement between results obtained comparing our and DDA calculations.

15. SUBJECT TERMS
Light scattering, Arbitrary particles, T-matrix, Sh-matrix

16. SECURITY CLASSIFICATION OF:			17. LIMITATION OF ABSTRACT	18. NUMBER OF PAGES	19a. NAME OF RESPONSIBLE PERSON
					GordenVideen
a. REPORT	b. ABSTRACT	c. THIS PAGE			19b. TELEPHONE NUMBER *(Include area code)*
Unclassified	Unclassified	Unclassified	UU	16	(301) 394-1871

Standard Form 298 (Rev. 8/98)
Prescribed by ANSI Std. Z39.18

Journal of Quantitative Spectroscopy & Radiative Transfer 112 (2011) 1636–1645

Contents lists available at ScienceDirect

Journal of Quantitative Spectroscopy & Radiative Transfer

journal homepage: www.elsevier.com/locate/jqsrt

Electromagnetic wave scattering from particles of arbitrary shapes

Dmitry Petrov [a,1], Yuriy Shkuratov [a], Gorden Videen [b,*]

[a] Astronomical Institute of Kharkov V.N. Karazin National University, 35 Sumskaya St, Kharkov 61022, Ukraine
[b] Army Research Laboratory RDRL-CIE-S, 2800 Powder Mill Road Adelphi, MD 20783, USA

ARTICLE INFO

Available online 4 February 2011

Keywords:
Light scattering
Arbitrary particles
T-matrix
Sh-matrix

ABSTRACT

We consider a general solution of the electromagnetic wave scattering problem for arbitrarily shaped homogeneous particles, whose surface can be expressed by a function of angular coordinates, using a Laplace series expansion. This can include regularly shaped particles (e.g., ellipsoids and cubes) as well as irregularly shaped particles like Gaussian spheres. For calculations of scattering properties of the particles, we use the approach based on the *Sh*-matrix. The *Sh*-matrix elements deduced from the *T*-matrix technique allow one to separate the shape effects from size- and refractive-index-dependent parameters. The separation also allows the corresponding surface integrals to be solved analytically for different particle shapes. In this manuscript, we give analytical expressions for the *Sh*-matrix elements for arbitrary shaped particles that can be presented with Laplace series. We find good agreement between results obtained comparing our and DDA calculations.

Published by Elsevier Ltd.

1. Introduction

One of the most fundamental characteristics that determine the scattering of electromagnetic waves from physical objects is the morphology of the objects. Within the last few decades, there have been many tantalizing studies of light scattering of electromagnetic waves as a function of particle shape, and significant progress has been achieved in the development of different algorithms and techniques in electromagnetic wave scattering [e.g., [1]]. These studies support applications in different fields of science and engineering from radar identification of satellites and airplanes to health assessment through the analysis of erythrocyte changes, due to the presence of diseases.

For scattering particles, the incident and scattered electromagnetic fields can be expressed as a superposition of vector harmonics, and the boundary conditions at interfaces can be satisfied exactly using analytical expressions. The scattered and incident vector harmonics are related through a *T*-matrix. For particles of complicated shapes, e.g., spheroids and Chebyshev particles, the *T*-matrix is typically found using a numerical technique. The primary advantage of such techniques is that light-scattering properties can be calculated relatively quickly. The disadvantage is that a separate algorithm is required for each particle shape. In numerical techniques, like the Discrete Dipole Approximation (DDA) and the Finite-Difference Time-Domain (FDTD) algorithms, the particle is discretized, so the shape is completely arbitrary and generally a single algorithm can handle all particle morphologies, including heterogeneities; however, these numerical methods can be cost prohibitive to run, especially when performing orientation averaging.

Recently, the shape matrix (or *Sh*-matrix) approach was developed within the extended boundary condition method (EBCM) of the *T*-matrix to facilitate the treatment of different morphologies [2]. The *Sh*-matrix elements depend only on particle shape and are found by performing corresponding surface integrals. Size and refractive index dependences are incorporated through analytical

* Corresponding author.
E-mail addresses: petrov@astron.kharkov.ua (D. Petrov), gorden.videen@gmail.com, gvideen@arl.army.mil (G. Videen).
[1] Tel.: +38 057 707 50 63.

0022-4073/$ - see front matter Published by Elsevier Ltd.
doi:10.1016/j.jqsrt.2011.01.036

operations on the *Sh*-matrix to produce the *T*-matrix. We have found that the *Sh*-matrix elements can be determined analytically for many types of particles, e.g., Chebyshev particles [3], capsule and bi-sphere particles [4], finite circular cylinders [5], corrugated finite cylinders and capsules [6], two merging spheres [7], small lenses [8], finite cylinders containing a spherical cavity [9], cuboid-like particles [10,11], merging spheroids [12], etc. All these particle shapes as well as many others can be described in a unified general approach that we present below.

Unfortunately, while algorithms exist to calculate the light scattering from virtually any type of particle, there has been a technology gap in characterizing the particles themselves, as shapes of most particles in nature cannot be described analytically by simple means. Our approach presented in this paper allows a simplification and unification of their morphological description. We combine this particle description with a *T*-matrix algorithm to calculate the light-scattering from arbitrary particles, using the *Sh*-matrix. We here offer: (1) a universal particle generation technique based on Laplace series; (2) expressions for *Sh*-matrix elements that are used to describe the *T*-matrix; and (3) several examples of electromagnetic wave scattering calculations using the *Sh*-matrix. It should be emphasized that a significant simplification in the computation of the electromagnetic wave scattering by particles results when applying the *Sh*-matrix to obtain analytical prescriptions.

2. Describing shape

Let us consider a particle whose shape is described by a single-valued continuous function $R(\theta,\varphi)$, where θ and φ are the polar and azimuth angles, respectively, in a spherical coordinate system with the center located within the particle. In our approach, we present $R(\theta,\varphi)$ as an expansion into the Laplace series using trigonometric functions and associated Legendre's polynomials

$$R(\theta,\varphi)=\sum_{l=0}^{\infty}\sum_{m=0}^{l}P_l^m(\cos\theta)(a_{lm}\cos m\varphi+b_{lm}\sin m\varphi) \quad (1)$$

where $P_l^m(x)$ are the associated Legendre polynomials. The coefficients a_{lm} and b_{lm} determine the particle shape. The series (1) is well known as the spherical functions expansion. The functions $P_l^m(\cos\theta)\cos m\varphi$ and $P_l^m(\cos\theta)\sin m\varphi$ (spherical harmonics) are a complete set of orthogonal functions and, thus, the set forms an orthonormal basis of the Hilbert space of square-integrable functions. On the unit sphere, any square-integrable function can thus be expanded as a linear combination of the functions. This expansion holds in the sense of the mean-square convergence, which says that

$$\lim_{N\to\infty}\int_0^{\pi}d\theta\sin\theta\int_0^{2\pi}d\varphi\left|R(\theta,\varphi)-\sum_{l=0}^{N}\sum_{m=0}^{l}P_l^m(\cos\theta)\left[a_{lm}\cos m\varphi+b_{lm}\sin m\varphi\right]\right|^2=0. \quad (2)$$

To apply the expansion in practice, the number N of series terms is finite, i.e. we imply that there is a finite N for which the following approximate expression can be considered as strict

$$R(\theta,\varphi)=\sum_{l=0}^{N}\sum_{m=0}^{l}P_l^m(\cos\theta)\left[a_{lm}\cos m\varphi+b_{lm}\sin m\varphi\right]. \quad (3)$$

The coefficients of expansion a_{lm} and b_{lm} can be found, if the function $R(\theta_i,\varphi_j)$ is known

$$a_{lm}=\frac{2l+1}{2\pi\varsigma_l}\frac{(l-m)!}{(l+m)!}\int_{-\pi/2}^{\pi/2}d\theta\sin\theta\int_0^{2\pi}d\phi\, R(\theta,\varphi)P_l^m(\cos\theta)\cos m\varphi, \quad (4)$$

$$b_{lm}=\frac{2l+1}{2\pi}\frac{(l-m)!}{(l+m)!}\int_{-\pi/2}^{\pi/2}d\theta\sin\theta\int_0^{2\pi}d\varphi\, R(\theta,\varphi)P_l^m(\cos\theta)\sin m\varphi, \quad (5)$$

where $\varsigma_0=2$ and $\varsigma_l=1$, if $l\neq 0$.

There is another way (skeleton method) to find coefficients using discrete values of the function $R(\theta_i,\varphi_j)$. Let us consider values at $2N^2$ points: $R_{ij}=R(\theta_i,\varphi_j)$, $i=1,\ldots,N$; $j=1,\ldots,2N$. By substituting $R(\theta_i,\varphi_j)$ into Eq. (3), we obtain a system of linear equations, where a_{lm} and b_{lm} are unknown. The solution of the system of linear equations gives us a representation of the particle shape as a simple and easily calculated expansion into a series expansion over trigonometric functions and associated Legendre's polynomials. Such an approach does not require an explicit form of the function $R(\theta,\varphi)$; it is sufficient to designate its values in $2N^2$ points. For example, one can generate numerically a group of radial vectors radiating more-or-less isotropically from the center of the spherical coordinate system. These vectors can be considered as a skeleton of a model particle. The length distribution of these vectors and orientation of each are arbitrary, depending on which particle one generates.

Thus, our approach can include regular particles (e.g., spheroids, ellipsoids and cubes) as well as particles with random shapes, like random Gaussian spheres [13,14]. Examples of model particles can be found in Figs. 1–6, where we also give intensity and polarization degree indicatrices. Unfortunately, this approach may not consider functions $R(\theta,\varphi)$ that are not continuous and single-valued. By this restriction our approach yields to numerical techniques like the DDA or FDTD methods.

We compare below results obtained for particles approximately generated by Eq. (3) and described with exact equations. These include ellipsoids, parallelepiped, erythrocyte-like particle, merged spheroids, and random Gaussian particles. In the case of ellipsoids, the function $R(\theta,\varphi)$ can be described using the approximation to cuboids [11]. Such a cuboid-like particle can be described using the function $R(\theta,\varphi)$ as follows:

$$R(\theta,\varphi)=\left[(\sin\theta)^{2n_0}\left[\left(\frac{\cos\varphi}{a}\right)^{2n_0}+\left(\frac{\sin\varphi}{b}\right)^{2n_0}\right]+\left(\frac{\cos\theta}{c}\right)^{2n_0}\right]^{-1/(2n_0)}, \quad (6)$$

where a, b, c are the cuboid hemi-axes, and n_0 defines the proximity of the cuboid-like particle to a pure parallelepiped. Note that at $n_0=1$, Eq. (6) describes the shape of an ellipsoid.

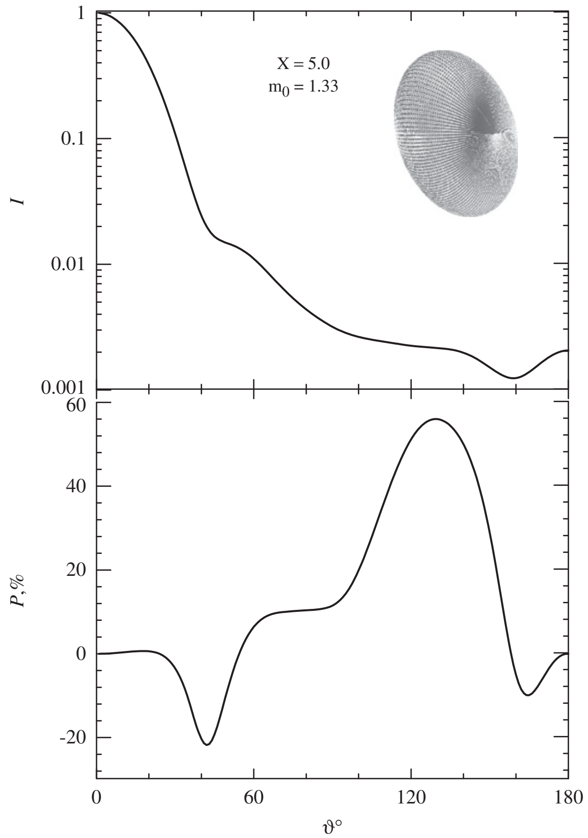

Fig. 1. Dependence of intensity (upper panel) and polarization degree (lower panel) on scattering angle for an approximated ellipsoid having the following hemi-axes a=1, b=0.75 and c=0.5, at m_0=1.33.

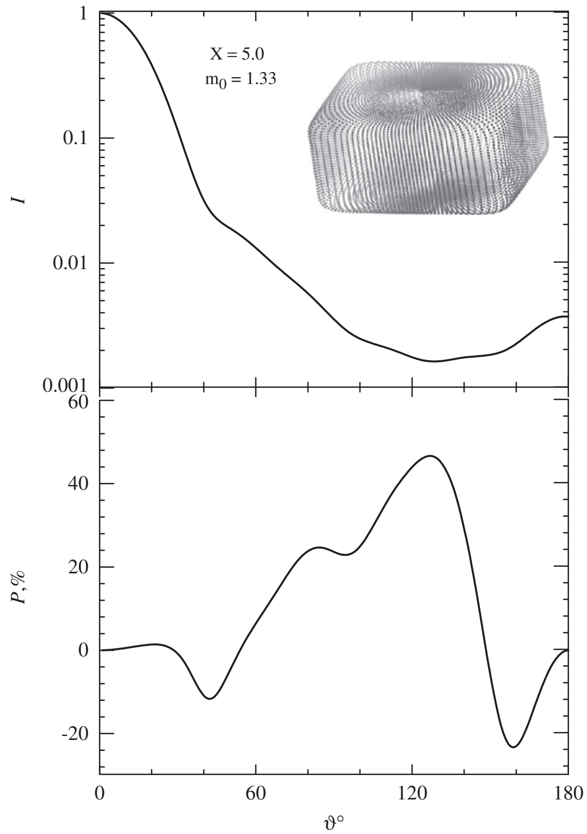

Fig. 2. Dependence of intensity (upper panel) and polarization degree (lower panel) on scattering angle for a parallelepiped-like particle with n_0=5, m_0=1.33, and a=1, b=0.75 and c=0.5.

The shape of the same merged spheres is described by the following equation:

$$R(\theta) = \sqrt{1+\mu\cos 2\theta}, \tag{7}$$

where μ is the parameter of merging, $0 \le \mu < 1$. At μ=0, the particle is a sphere and at $\mu \to 1$ the particle is a bi-sphere.

Gaussian random spheres are described through the spherical harmonics and the associated Legendre polynomials in the following manner [13,14]:

$$R(\theta,\,\varphi) = \frac{Ce^{S(\theta,\,\varphi)}}{\sqrt{1+\sigma^2}}, \tag{8}$$

where C is a normalized constant and

$$S(\theta,\,\varphi) = \sum_{l=0}^{\infty}\sum_{m=0}^{l} P_l^m(\cos\theta)\left(\tilde{a}_{lm}\cos m\varphi + \tilde{b}_{lm}\sin m\varphi\right), \tag{9}$$

where coefficients $\tilde{a}_{lm}$ and $\tilde{b}_{lm}$ are independent Gaussian random variables with zero mean and variances that depend on indices l and m as follows:

$$\beta_{lm}^2 = (2-\delta_{m0})\frac{(2l+1)(l-m)!}{(l+m)!}\exp(-\kappa)i_l(\kappa)\ln(1+\sigma^2), \tag{10}$$

$$\kappa = \frac{1}{4}\left(\sin\frac{\Gamma}{2}\right)^{-2}, \tag{11}$$

where σ^2 is the radii variance, Γ is the correlation angle and $i_l(\kappa)$ are the modified spherical Bessel functions. This method allows generation of irregular particles with the parameters σ and Γ; usually $\Gamma > 3^\circ$.

3. *Sh*-matrices and their relation to the *T*-matrix

Within the T-matrix method, the incident and scattered fields are expanded in a series of appropriate vector spherical functions [1]

$$E^{inc}(r,\,\gamma,\,\phi) = \sum_{n=1}^{\infty}\sum_{m=-n}^{n}\left[p_{mn}^{inc}RgM_{mn}(r,\,\gamma,\,\phi) + q_{mn}^{inc}RgN_{mn}(r,\,\gamma,\,\phi)\right], \tag{12}$$

$$E^{sca}(r,\,\gamma,\,\phi) = \sum_{n=1}^{\infty}\sum_{m=-n}^{n}\left[p_{mn}^{sca}M_{mn}(r,\,\gamma,\,\phi) + q_{mn}^{sca}N_{mn}(r,\,\gamma,\,\phi)\right], \tag{13}$$

where Rg$\boldsymbol{M}_{mn}(r,\gamma,\phi)$, Rg$\boldsymbol{N}_{mn}(r,\gamma,\phi)$, $\boldsymbol{M}_{mn}(r,\gamma,\phi)$, $\boldsymbol{N}_{mn}(r,\gamma,\phi)$ and p_{mn}^{inc}, q_{mn}^{inc}, p_{mn}^{sca} and q_{mn}^{sca} are the vector spherical functions and corresponding expansion coefficients, r is the distance from the coordinate center (the particle center) and γ and ϕ are the polar and azimuth angles,

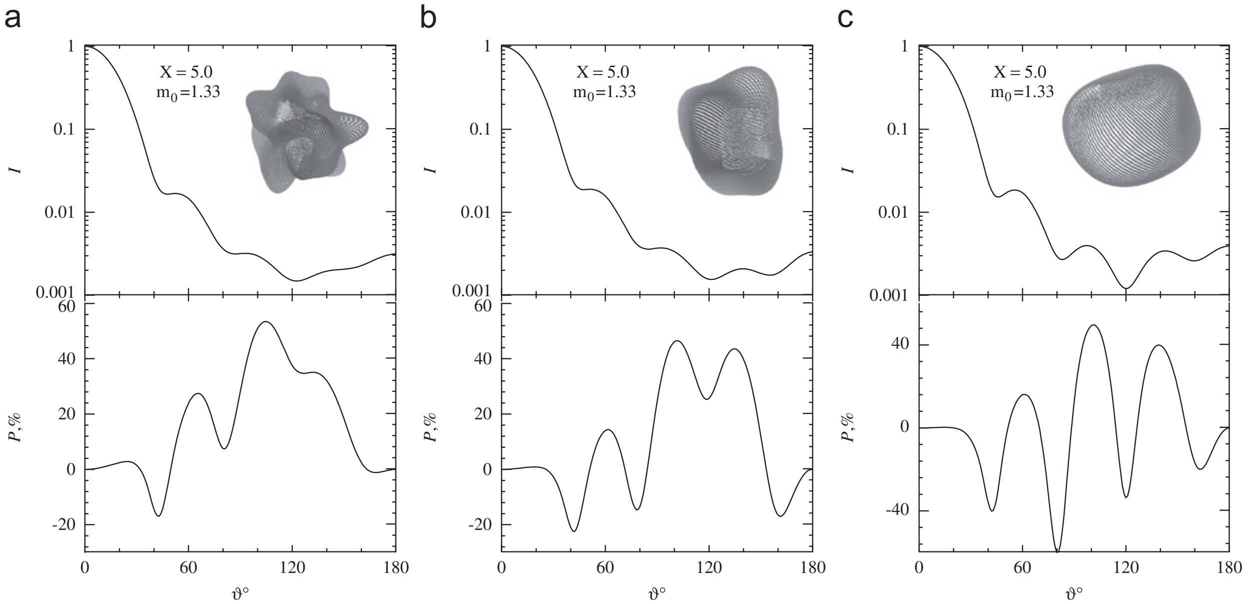

Fig. 3. Dependence of intensity (upper panel) and polarization degree (lower panel) on scattering angle for an approximated Gaussian sphere having σ=0.3 and Γ=10° (a), Γ=30° (b), Γ=50° (c) at m_0=1.33.

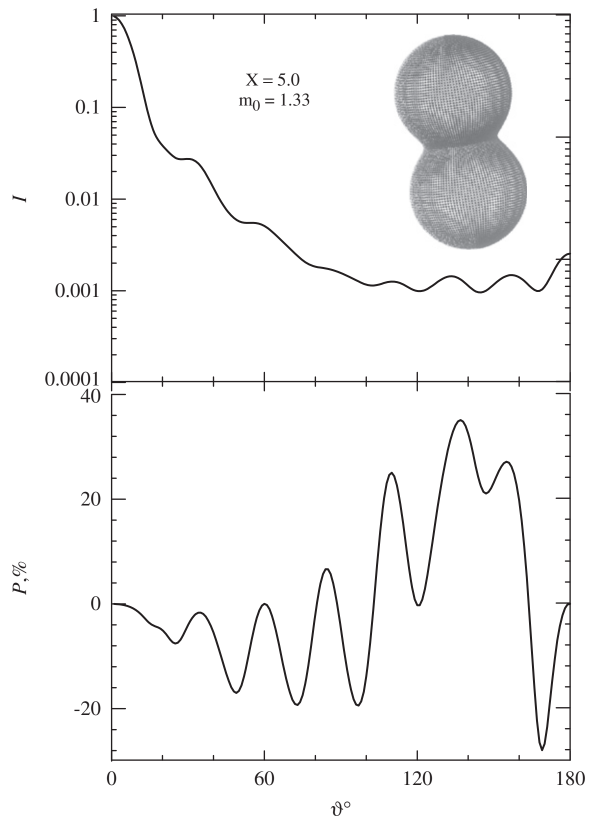

Fig. 4. Dependence of intensity (upper panel) and polarization degree (lower panel) on scattering angle for an approximated merged sphere with μ=0.8 and m_0=1.33.

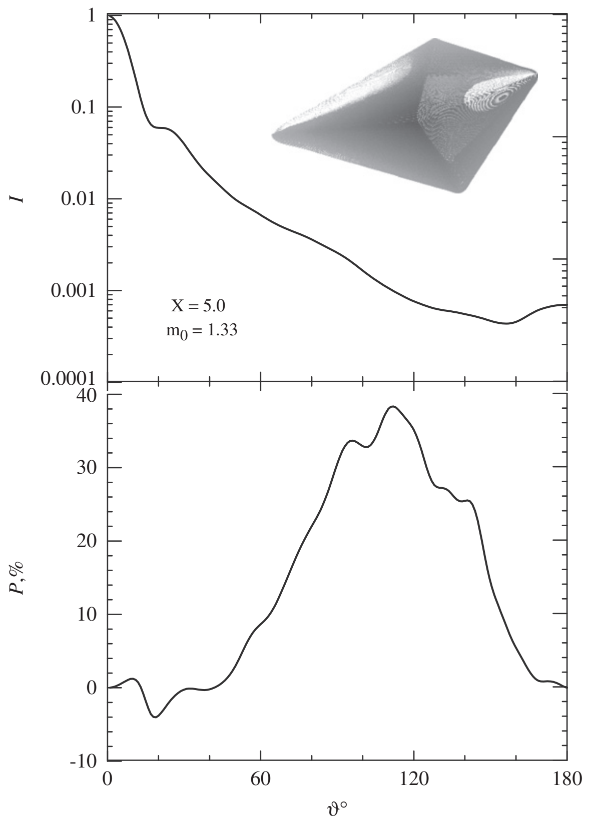

Fig. 5. Dependence of intensity (upper panel) and polarization degree (lower panel) on scattering angle for an arbitrary hexahedron generated by Eq. (3) with m_0=1.33.

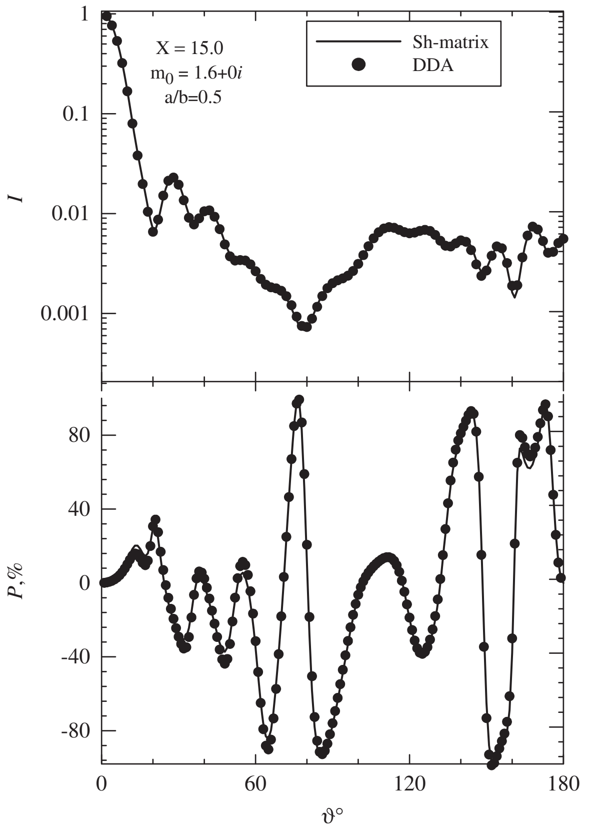

Fig. 6. Comparison between *Sh*-matrix and DDA calculations for an oblate spheroid averaged over orientations. For DDA calculations are from the code of Zubko [17].

respectively, that are used to characterize the scattering geometry. The functions $\mathrm{Rg}\boldsymbol{M}_{mn}(r,\gamma,\phi)$ and $\mathrm{Rg}\boldsymbol{N}_{mn}(r,\gamma,\phi)$ are finite in the coordinate center (Rg(…) means "Regular"). The explicit expressions for the vector spherical wave functions are given, e.g., in [1]. The coefficients p_{mn}, q_{mn} relate to a_{mn}, b_{mn} as follows [1]:

$$p_{mn}^{sca} = \sum_{n'=1}^{\infty} \sum_{m'=-n'}^{n'} \left[T_{mnm'n'}^{11} p_{m'n'}^{inc} + T_{mnm'n'}^{12} q_{m'n'}^{inc} \right], \tag{14}$$

$$q_{mn}^{sca} = \sum_{n'=1}^{\infty} \sum_{m'=-n'}^{n'} \left[T_{mnm'n'}^{21} p_{m'n'}^{inc} + T_{mnm'n'}^{22} q_{m'n'}^{inc} \right]. \tag{15}$$

The *T*-matrix

$$T_{mnm'n'} = \begin{pmatrix} T_{mnm'n'}^{11} & T_{mnm'n'}^{12} \\ T_{mnm'n'}^{21} & T_{mnm'n'}^{22} \end{pmatrix}. \tag{16}$$

can be presented [1] as

$$T_{mnm'n'} = -(\mathrm{Rg}Q_{mnm'n'})(Q_{mnm'n'})^{-1}, \tag{17}$$

The matrices $\mathrm{Rg}\boldsymbol{Q}_{mnm'n'}$ and $\boldsymbol{Q}_{mnm'n'}$ are

$$Q_{mnm'n'} = -i \begin{pmatrix} m_0 J_{mnm'n'}^{21} + J_{mnm'n'}^{12} & m_0 J_{mnm'n'}^{11} + J_{mnm'n'}^{22} \\ m_0 J_{mnm'n'}^{22} + J_{mnm'n'}^{11} & m_0 J_{mnm'n'}^{12} + J_{mnm'n'}^{21} \end{pmatrix}, \tag{18}$$

$$\mathrm{Rg}Q_{mnm'n'} = -i \begin{pmatrix} m_0 \mathrm{Rg}J_{mnm'n'}^{21} + \mathrm{Rg}J_{mnm'n'}^{12} & m_0 \mathrm{Rg}J_{mnm'n'}^{11} + \mathrm{Rg}J_{mnm'n'}^{22} \\ m_0 \mathrm{Rg}J_{mnm'n'}^{22} + \mathrm{Rg}J_{mnm'n'}^{11} & m_0 \mathrm{Rg}J_{mnm'n'}^{12} + \mathrm{Rg}J_{mnm'n'}^{21} \end{pmatrix}, \tag{19}$$

where the values $J_{mnm'n'}^{11}$, $J_{mnm'n'}^{12}$, $J_{mnm'n'}^{21}$, $J_{mnm'n'}^{22}$ and $\mathrm{Rg}J_{mnm'n'}^{11}$, $\mathrm{Rg}J_{mnm'n'}^{12}$, $\mathrm{Rg}J_{mnm'n'}^{21}$, $\mathrm{Rg}J_{mnm'n'}^{22}$ can be expressed through integrals over the particle surface [1]; corresponding expressions are very cumbersome and we here omit them. We modify the integrals, introducing the *Sh*-matrices [2]. The central point of the *Sh*-matrix derivation is the multiplication theorem for Bessel functions $j_\nu(z)$ [15]

$$j_\nu(cz) = c^\nu \sum_{k=0}^{\infty} \frac{(-1)^k (c^2-1)^k \left(\frac{z}{2}\right)^k}{k!} j_{\nu+k}(z), \tag{20}$$

where c is here an arbitrary number. This allows one to retrieve multipliers m_0X and X from arguments $m_0X\rho$ and $X\rho$, where $\rho = R(\theta,\varphi)/X$ is the normalized shape function, m_0 is the complex refractive index and $X = 2\pi R_0/\lambda$ is the size parameter, R_0 and λ are the characteristic particle size (e.g., the size of the major axis of a particle or the size parameter of the sphere of the equivalent volume) and the wavelength of the incident light, respectively. Thus, we separate the influence of the particle shape and parameters X and m_0, introducing the *Sh*-matrices [2]

$$\mathrm{Rg}J_{mnm'n'}^{11}(X, m_0) = X^{n+n'+2} (m_0)^{n'} \sum_{k_1=0}^{\infty} \Psi_1 \sum_{k_2=0}^{\infty} \Psi_2 \mathrm{Rg}Sh_{mnm'n',\,k_1+k_2}^{11}, \tag{21}$$

$$\mathrm{Rg}J_{mnm'n'}^{12}(X, m_0) = X^{n+n'+1} (m_0)^{n'} \sum_{k_1=0}^{\infty} \Psi_1 \sum_{k_2=0}^{\infty} \Psi_2 \left(\mathrm{Rg}Sh_{mnm'n',\,k_1+k_2}^{121} + \chi_2 \mathrm{Rg}Sh_{mnm'n',\,k_1+k_2}^{122} \right), \tag{22}$$

$$\mathrm{Rg}J_{mnm'n'}^{21}(X, m_0) = X^{n+n'+1} (m_0)^{n'-1} \sum_{k_1=0}^{\infty} \Psi_1 \sum_{k_2=0}^{\infty} \Psi_2 \left(\mathrm{Rg}Sh_{mnm'n',k_1+k_2}^{211} + \chi_1 \mathrm{Rg}Sh_{mnm'n',k_1+k_2}^{212} \right), \tag{23}$$

$$\mathrm{Rg}J_{mnm'n'}^{22}(X, m_0) = X^{n+n'} (m_0)^{n'-1} \sum_{k_1=0}^{\infty} \Psi_1 \sum_{k_2=0}^{\infty} \Psi_2 \left(\mathrm{Rg}Sh_{mnm'n',\,k_1+k_2}^{221} + \chi_1 \mathrm{Rg}Sh_{mnm'n',\,k_1+k_2}^{222} + \chi_2 \mathrm{Rg}Sh_{mnm'n',\,k_1+k_2}^{223} + \chi_1\chi_2 \mathrm{Rg}Sh_{mnm'n',\,k_1+k_2}^{224} \right), \tag{24}$$

$$J_{mnm'n'}^{11}(X, m_0) = \mathrm{Rg}J_{mnm'n'}^{11}(X, m_0) + X^{n'-n+1} (m_0)^{n'} \sum_{k_1=0}^{\infty} \Psi_1 \sum_{k_2=0}^{\infty} \Psi_3 Sh_{mnm'n',\,k_1+k_2}^{11}, \tag{25}$$

$$J_{mnm'n'}^{12}(X, m_0) = \mathrm{Rg}J_{mnm'n'}^{12}(X, m_0) + X^{n'-n} (m_0)^{n'} \sum_{k_1=0}^{\infty} \Psi_1 \sum_{k_2=0}^{\infty} \Psi_3 \left(Sh_{mnm'n',\,k_1+k_2}^{121} + \chi_3 Sh_{mnm'n',\,k_1+k_2}^{122} \right), \tag{26}$$

$$J^{21}_{mnm'n'}(X, m_0) = \mathrm{Rg}J^{21}_{mnm'n'}(X, m_0) + X^{n'-n}(m_0)^{n'-1}\sum_{k_1=0}^{\infty} \Psi_1 \sum_{k_2=0}^{\infty} \Psi_3 \left(Sh^{211}_{mnm'n',\, k_1+k_2} + \chi_1 Sh^{212}_{mnm'n',\, k_1+k_2} \right), \tag{27}$$

$$J^{22}_{mnm'n'}(X, m_0) = \mathrm{Rg}J^{22}_{mnm'n'}(X, m_0) + X^{n'-n-1}(m_0)^{n'-1} \sum_{k_1=0}^{\infty} \Psi_1 \sum_{k_2=0}^{\infty} \Psi_3 \left(Sh^{221}_{mnm'n',\, k_1+k_2} + \chi_1 Sh^{222}_{mnm'n',\, k_1+k_2} + \chi_3 Sh^{223}_{mnm'n',\, k_1+k_2} + \chi_1\chi_3 Sh^{224}_{mnm'n',\, k_1+k_2} \right), \tag{28}$$

where $\chi_1 = (Xm_0)^2/(n'+k_1+3/2)$, $\chi_2 = X^2/(n+k_2+3/2)$, $\chi_3 = X^2/(k_2-n+1/2)$, $\Psi_1 = (Xm_0)^{2k_1}/(k_1!\Gamma(n'+k_1+3/2))$, $\Psi_2 = X^{2k_2}/(k_2!\Gamma(n+k_2+3/2))$ and $\Psi_3 = X^{2k_2}/(k_2!\Gamma(k_2-n+1/2))$. The explicit expressions for the *Sh*-matrices accounting for the expansion (3) are presented in Appendix. It should be emphasized that the *Sh*-matrices have no deep physical sense, like the *T*-matrix; these are designations of corresponding surface integrals that do not depend on the parameters m_0 and X.

We note that in practice the infinite limits in Eqs. (12) and (13) should be finite n_{min}; this number depends on the required accuracy, but it increases with X and is a function of particle shape as we discuss below.

The matrix $\boldsymbol{T}_{mnm'n'}$ depends only on the optical and morphological characteristics of a scattering particle such as the complex refractive index m_0 and the size parameter X. This matrix is independent of the particle illumination/observation geometry and incident light polarization, i.e. the matrix once computed may be exploited for any illumination geometry and polarization. Similarly the *Sh*-matrices are independent of m_0 and X and once computed, they can be used to calculate the *T*-matrix for any m_0 and X.

4. Calculations and discussion

We examine the light scattering for some particle shapes generated by the skeleton method with Eq. (3) at different m_0 and X (the size parameter of a sphere of an equivalent volume).

Table 1 shows values of the minimal number of terms N_m in Eq. (3) needed to represent the particles within 0.5% (X=10 and m_0=1.5+0i); i.e. the maximal difference between the real particle radial vector R and its expansion should be not more than 0.5%. As can be anticipated, the description of an ellipsoid requires the fewest terms, and the description of a cuboid-like particle requires the most terms.

Table 2 shows the computation time as a function of the number of expansion terms in Eqs. (3), (12) and (13) for cube-like particles approximated by Eq. (3) at n_0=10, with X=10, and m_0=1.5+0i. With increasing N in Eq. (3), calculation time quickly increases. The parameter n_{min} means the minimal number of expansion terms in Eqs. (12) and (13) needed to provide 0.5% accuracy of calculation of *T*-matrix elements. The difference between neighbor values of the elements was used for the accuracy estimate. The parameter n_{min} depends on many different factors; in particular, it is a function of N and X.

In Figs. 1–5, we show the dependence of intensity and polarization degree on the scattering angle ϑ. They were calculated with the *Sh*-matrices (see Appendix) for particles of different shape; excepting shape, all particle parameters are the same X=5 and m_0=1.33+0i. As one can see, shape plays a very important role in forming scattering properties even for small X. It is interesting to note that all oblong particles have a prominent negative polarization branch at small phase angles (large scattering angles). Almost all particles display negative polarization at small ϑ, which is observed for very large particles when the geometrical optics approximation is valid (e.g., [16]). Figs. 1 and 2 depict curves for an approximated ellipsoid having hemi-axes a=1, b=0.75, c=0.5 (n_0=1 in Eq. (6)) and for an approximated parallelepiped-like particle having the same parameters and n_0=5. Curves corresponding to n_0=1 and 5 are rather similar, although the negative polarization at large ϑ has a deeper branch when n_0=5. Fig. 3 shows curves for a random Gaussian sphere having σ=0.3 and Γ=10° (a), 30° (b) and 50° (c). As can be anticipated, when the shape tends to a sphere, the particles demonstrate more complicated $I(\vartheta)$ and $P(\vartheta)$, due to the preservation of the morphology-dependent resonance structure. Fig. 4 shows curves for merged spheres at μ=0.8; this particle shows the most complicated structure of $I(\vartheta)$ and $P(\vartheta)$, which is related to the interference between the two components making up the structure. For Figs. 1–4, we made calculations using the shapes generated with exact equations and approximations found with Eq. (3). In all cases, we observed the coincidence of approximate and exact $I(\vartheta)$ and $P(\vartheta)$ within the thickness of curves on figures. Fig. 5 shows curves for an arbitrary hexahedron generated with Eq. (3) also by the skeleton method, as shown in the inset. In this case, the functions $I(\vartheta)$ and $P(\vartheta)$ show relatively little structure.

Table 2
Time of calculation and the minimal number of required terms in the *Sh*-matrices for calculation of scattering (relative error is < 0.5%) for a cube-like particle (n_0=10, X=10 and m_0=1.5+0i) as a function of N in Eq. (3).

n_{min}	22	24	26	27	28	30	31
N	20	30	40	50	60	70	80
Time (s)	4	12	27	59	132	285	536

Table 1
Minimal number of expansion terms N_m needed for the representation of particle shape with an accuracy of 0.5% (X=10 and m_0=1.5+0i).

Type	Ellipsoids			Parallelepiped-like particles (n_0=5)			Gaussian particles, Γ		
	$a=b=2c$	$a=b=c/2$	$a=2b=c/2$	$a=b=2c$	$a=b=c/2$	$a=2b=c/2$	20°	40°	60°
N_m	12	16	18	26	32	38	20	28	32

We compare *Sh*-matrix and DDA calculations for many different shapes. Fig. 6 shows one example—results for an oblate spheroid averaged over orientation. For DDA calculations, the validated code of Zubko [17] was used. As one can see the difference between curves calculated by the different techniques are negligibly small. We have made the same kind of comparison many times earlier in [2–8], demonstrating excellent coincidence for a variety of shapes.

5. Conclusion

In this article, we have provided a new general algorithm for calculating the light scattered by homogeneous particles, whose shape can be described by a single-valued continuous function $R(\theta,\varphi)$. Such an algorithm provides an alternative to the DDA and FDTD algorithms that are typically used to calculate the light scattered from irregular particles. Within the algorithm, the particle morphology is expressed in terms of a finite Laplace series. We calculate the *Sh*-matrix directly from coefficients of expansion of Laplace series using the analytical expressions provided in Appendix. The *Sh*-matrix contains all the morphological information, but does not contain information about the particle size or refractive index. The *T*-matrix, and subsequent light-scattering properties, is found directly from the *Sh*-matrix using analytical expressions that include the refractive index and size dependence; thus, the *Sh*-matrix only needs to be computed once for a class of particles of similar shape, but having different sizes or refractive indices.

Acknowledgments

This work was supported by the Army Medical Research Institute of Chemical Defense (Lucille Lumley, Ph.D.) under the auspices of the U.S. Army Research Office Scientific Services Program administered by Battelle (Delivery Order 0378, Contract no. W911NF-07-D-0001). The authors thank E. Zubko for the use of his DDA code.

Appendix

The *Sh*-matrix elements are expressed as follows:

$$\mathrm{Rg}Sh^{11}_{mnm'n',\,k} = -\pi i \frac{(-1)^{m'-m+k}}{2^{2k+n'+n+2}} A_{nn'} \sum_{l=0}^{\infty} \sum_{q=0}^{l} \left[I^{(1)}_{mnm'n'}(q,\,l,\,2k+n+n'+2) \Phi^{(0)}_{m'-m}(q,\,l,\,0,\,0,\,2k+n+n'+2) \right], \tag{A1}$$

$$\mathrm{Rg}Sh^{121}_{mnm'n',\,k} = \pi \frac{(-1)^{m'-m+k}}{2^{2k+n'+n+2}} A_{nn'} \sum_{l=0}^{\infty} \sum_{q=0}^{l} \left[\begin{array}{l} (n+1) I^{(2)}_{mnm'n'}(q,\,l,\,2k+n+n'+1) \Phi^{(0)}_{m'-m}(q,\,l,\,0,\,0,\,2k+n+n'+1) + \\ \displaystyle\sum_{l'=0}^{\infty} \sum_{k'=0}^{l'} \left[\begin{array}{l} L^{(01)}_{mnm'n'}(q,\,l,\,k',\,l',\,2k+n+n') \Phi^{(0)}_{m'-m}(q,\,l,\,k',\,l',\,2k+n+n'+1) + \\ +iL^{(10)}_{mnm'n'}(q,\,l,\,2k+n+n'+1) \Phi^{(1)}_{m'-m}(q,\,l,\,k',\,l',\,2k+n+n') \end{array} \right] \end{array} \right], \tag{A2}$$

$$\mathrm{Rg}Sh^{122}_{mnm'n',\,k} = -\pi \frac{(-1)^{m'-m+k}}{2^{2k+n'+n+3}} A_{nn'} \sum_{l=0}^{\infty} \sum_{q=0}^{l} \left[I^{(2)}_{mnm'n'}(q,\,l,\,2k+n+n'+3) \Phi^{(0)}_{m'-m}(q,\,l,\,0,\,0,\,2k+n+n'+3) \right], \tag{A3}$$

$$\mathrm{Rg}Sh^{211}_{mnm'n',\,k} = -\pi \frac{(-1)^{m'-m+k}}{2^{2k+n'+n+2}} A_{nn'} \sum_{l=0}^{\infty} \sum_{q=0}^{l} \left[\begin{array}{l} (n'+1) I^{(2)}_{mnm'n'}(q,\,l,\,2k+n+n'+1) \Phi^{(0)}_{m'-m}(q,\,l,\,0,\,0,\,2k+n+n'+1) + \\ \displaystyle\sum_{l'=0}^{\infty} \sum_{k'=0}^{l'} \left[\begin{array}{l} +L^{(01)}_{m'n'mn}(q,\,l,\,k',\,l',\,2k+n+n') \Phi^{(0)}_{m'-m}(q,\,l,\,k',\,l',\,2k+n+n'+1) - \\ -iL^{(10)}_{m'n'mn}(q,\,l,\,2k+n+n'+1) \Phi^{(1)}_{m'-m}(q,\,l,\,k',\,l',\,2k+n+n') \end{array} \right] \end{array} \right] \tag{A4}$$

$$\mathrm{Rg}Sh^{212}_{mnm'n',\,k} = \pi \frac{(-1)^{m'-m+k}}{2^{2k+n'+n+3}} A_{nn'} \sum_{l=0}^{\infty} \sum_{q=0}^{l} \left[I^{(2)}_{mnm'n'}(q,\,l,\,2k+n+n'+3) \Phi^{(0)}_{m'-m}(q,\,l,\,0,\,0,\,2k+n+n'+3) \right], \tag{A5}$$

$$\mathrm{Rg}Sh^{221}_{mnm'n',\,k} = -i\pi \frac{(-1)^{m'-m+k}}{2^{2k+n'+n+2}} A_{nn'} \sum_{l=0}^{\infty} \sum_{q=0}^{l} \left[\begin{array}{l} (n'+1)(n+1) I^{(1)}_{mnm'n'}(q,\,l,\,2k+n+n') \Phi^{(0)}_{m'-m}(q,\,l,\,0,\,0,\,2k+n+n') + \\ \displaystyle\sum_{l'=0}^{\infty} \sum_{k'=0}^{l'} \left[\begin{array}{l} +(n'+1) L^{(00)}_{mnm'n'}(q,\,l,\,k',\,l',\,2k+n+n'-1) \Phi^{(0)}_{m'-m}(q,\,l,\,k',\,l',\,2k+n+n') + \\ +i(n'+1) L^{(11)}_{mnm'n'}(q,\,l,\,2k+n+n') \Phi^{(1)}_{m'-m}(q,\,l,\,k',\,l',\,2k+n+n'-1) + \\ +(n+1) L^{(00)}_{m'n'mn}(q,\,l,\,k',\,l',\,2k+n+n'-1) \Phi^{(0)}_{m'-m}(q,\,l,\,k',\,l',\,2k+n+n') + \\ +i(n+1) L^{(11)}_{m'n'mn}(q,\,l,\,2k+n+n') \Phi^{(1)}_{m'-m}(q,\,l,\,k',\,l',\,2k+n+n'-1) \end{array} \right] \end{array} \right], \tag{A6}$$

$$\mathrm{Rg}Sh^{222}_{mnm'n',\,k} = i\pi\frac{(-1)^{m'-m+k}}{2^{2k+n'+n+3}}A_{nn'}\sum_{l=0}^{\infty}\sum_{q=0}^{l}\left[\begin{array}{l}(n+1)I^{(1)}_{mnm'n'}(q,l,2k+n+n'+2)\Phi^{(0)}_{m'-m}(q,l,0,0,2k+n+n'+2)+\\ \sum_{l'=0}^{\infty}\sum_{k'=0}^{l'}\left[\begin{array}{l}+L^{(00)}_{mnm'n'}(q,l,k',l',2k+n+n'+1)\Phi^{(0)}_{m'-m}(q,l,k',l',2k+n+n'+2)-\\ -iL^{(11)}_{mnm'n'}(q,l,2k+n+n'+2)\Phi^{(1)}_{m'-m}(q,l,k',l',2k+n+n'+1)\end{array}\right]\end{array}\right], \tag{A7}$$

$$\mathrm{Rg}Sh^{223}_{mnm'n',\,k} = i\pi\frac{(-1)^{m'-m+k}}{2^{2k+n'+n+3}}A_{nn'}\sum_{l=0}^{\infty}\sum_{q=0}^{l}\left[\begin{array}{l}(n'+1)I^{(1)}_{mnm'n'}(q,l,2k+n+n'+2)\Phi^{(0)}_{m'-m}(q,l,0,0,2k+n+n'+2)+\\ \sum_{l'=0}^{\infty}\sum_{k'=0}^{l'}\left[\begin{array}{l}+L^{(00)}_{m'n'mn}(q,l,k',l',2k+n+n'+1)\Phi^{(0)}_{m'-m}(q,l,k',l',2k+n+n'+2)-\\ -iL^{(11)}_{m'n'mn}(q,l,2k+n+n'+2)\Phi^{(1)}_{m'-m}(q,l,k',l',2k+n+n'+1)\end{array}\right]\end{array}\right], \tag{A8}$$

$$\mathrm{Rg}Sh^{224}_{mnm'n',\,k} = -i\pi\frac{(-1)^{m'-m+k}}{2^{2k+n'+n+4}}A_{nn'}\sum_{l=0}^{\infty}\sum_{q=0}^{l}\left[I^{(1)}_{mnm'n'}(q,l,2k+n+n'+4)\Phi^{(0)}_{m'-m}(q,l,0,0,2k+n+n'+4)\right], \tag{A9}$$

$$Sh^{11}_{mnm'n',\,k} = \pi\frac{(-1)^{m'-m+n-1+k}}{2^{2k+n'-n+1}}A_{nn'}\sum_{l=0}^{\infty}\sum_{q=0}^{l}\left[I^{(1)}_{mnm'n'}(q,l,2k-n+n'+1)\Phi^{(0)}_{m'-m}(q,l,0,0,2k-n+n'+1)\right], \tag{A10}$$

$$Sh^{121}_{mnm'n',\,k} = i\pi\frac{(-1)^{m'-m+n-1+k}}{2^{2k+n'-n+1}}A_{nn'}\sum_{l=0}^{\infty}\sum_{q=0}^{l}\left[\begin{array}{l}-nI^{(2)}_{mnm'n'}(q,l,2k-n+n')\Phi^{(0)}_{m'-m}(q,l,0,0,2k-n+n')+\\ \sum_{l'=0}^{\infty}\sum_{k'=0}^{l'}\left[\begin{array}{l}+L^{(01)}_{mnm'n'}(q,l,k',l',2k-n+n'-1)\Phi^{(0)}_{m'-m}(q,l,k',l',2k-n+n')+\\ +L^{(10)}_{mnm'n'}(q,l,2k-n+n')\Phi^{(1)}_{m'-m}(q,l,k',l',2k-n+n'-1)\end{array}\right]\end{array}\right], \tag{A11}$$

$$Sh^{122}_{mnm'n',\,k} = -i\pi\frac{(-1)^{m'-m-n+1+k}}{2^{2k+n'-n+2}}A_{nn'}\sum_{l=0}^{\infty}\sum_{q=0}^{l}\left[I^{(2)}_{mnm'n'}(q,l,2k-n+n'+2)\Phi^{(0)}_{m'-m}(q,l,0,0,2k-n+n'+2)\right], \tag{A12}$$

$$Sh^{211}_{mnm'n',\,k} = -i\pi\frac{(-1)^{m'-m-n-1+k}}{2^{2k+n'-n+1}}A_{nn'}\sum_{l=0}^{\infty}\sum_{q=0}^{l}\left[\begin{array}{l}(n'+1)I^{(2)}_{mnm'n'}(q,l,2k-n+n')\Phi^{(0)}_{m'-m}(q,l,0,0,2k-n+n')+\\ \sum_{l'=0}^{\infty}\sum_{k'=0}^{l'}\left[\begin{array}{l}L^{(00)}_{mnm'n'}(q,l,k',l',2k-n+n'-1)\Phi^{(0)}_{m'-m}(q,l,k',l',2k-n+n')-\\ -iL^{(11)}_{mnm'n'}(q,l,2k-n+n')\Phi^{(1)}_{m'-m}(q,l,k',l',2k-n+n'-1)\end{array}\right]\end{array}\right], \tag{A13}$$

$$Sh^{212}_{mnm'n',\,k} = i\pi\frac{(-1)^{m'-m-n-1+k}}{2^{2k+n'-n+1}}A_{nn'}\sum_{l=0}^{\infty}\sum_{q=0}^{l}\left[I^{(2)}_{mnm'n'}(q,l,2k-n+n'+2)\Phi^{(0)}_{m'-m}(q,l,0,0,2k-n+n'+2)\right], \tag{A14}$$

$$Sh^{221}_{mnm'n',\,k} = \frac{\pi(-1)^{m'-m-n-1+k}}{2^{2k+n'-n+1}}A_{nn'}\sum_{l=0}^{\infty}\sum_{q=0}^{l}\left[\begin{array}{l}-n(n'+1)I^{(1)}_{mnm'n'}(q,l,2k-n+n'-1)\Phi^{(0)}_{m'-m}(q,l,0,0,2k-n+n'-1)+\\ \sum_{l'=0}^{\infty}\sum_{k'=0}^{l'}\left[\begin{array}{l}(n'+1)L^{(00)}_{mnm'n'}(q,l,k',l',2k-n+n'-2)\Phi^{(0)}_{m'-m}(q,l,k',l',2k-n+n'-1)+\\ +i(n'+1)L^{(11)}_{mnm'n'}(q,l,2k-n+n'-1)\Phi^{(1)}_{m'-m}(q,l,k',l',2k-n+n'-2)-\\ -nL^{(00)}_{m'n'mn}(q,l,k',l',2k-n+n'-2)\Phi^{(0)}_{m'-m}(q,l,k',l',2k-n+n'-1)+\\ +inL^{(11)}_{m'n'mn}(q,l,2k-n+n'-1)\Phi^{(1)}_{m'-m}(q,l,k',l',2k-n+n'-2)\end{array}\right]\end{array}\right], \tag{A15}$$

$$Sh^{222}_{mnm'n',\,k} = -\pi\frac{(-1)^{m'-m-n-1+k}}{2^{2k+n'-n+2}}A_{nn'}\sum_{l=0}^{\infty}\sum_{q=0}^{l}\left[\begin{array}{l}-nI^{(1)}_{mnm'n'}(q,l,2k-n+n'+1)\Phi^{(0)}_{m'-m}(q,l,0,0,2k-n+n'+1)+\\ \sum_{l'=0}^{\infty}\sum_{k'=0}^{l'}\left[\begin{array}{l}L^{(00)}_{mnm'n'}(q,l,k',l',2k-n+n')\Phi^{(0)}_{m'-m}(q,l,k',l',2k-n+n'+1)+\\ +iL^{(11)}_{mnm'n'}(q,l,2k-n+n'+1)\Phi^{(1)}_{m'-m}(q,l,k',l',2k-n+n')\end{array}\right]\end{array}\right], \tag{A16}$$

$$Sh^{223}_{mnm'n',\,k} = \pi\frac{(-1)^{m'-m-n-1+k}}{2^{2k+n'-n+2}}A_{nn'}\sum_{l=0}^{\infty}\sum_{q=0}^{l}\left[\begin{array}{l}(n'+1)I^{(1)}_{mnm'n'}(q,l,2k-n+n'+1)\Phi^{(0)}_{m'-m}(q,l,0,0,2k-n+n'+1)+\\ \sum_{l'=0}^{\infty}\sum_{k'=0}^{l'}\left[\begin{array}{l}L^{(00)}_{m'n'mn}(q,l,k',l',2k-n+n')\Phi^{(0)}_{m'-m}(q,l,k',l',2k-n+n'+1)-\\ -iL^{(11)}_{m'n'mn}(q,l,2k-n+n'+1)\Phi^{(1)}_{m'-m}(q,l,k',l',2k-n+n')\end{array}\right]\end{array}\right], \tag{A17}$$

$$Sh^{224}_{mnm'n',\,k} = \pi\frac{(-1)^{m'-m-n+1+k}}{2^{2k+n'-n+3}}A_{nn'}\sum_{l=0}^{\infty}\sum_{q=0}^{l}\left[I^{(1)}_{mnm'n'}(q,\,l,\,2k-n+n'+3)\Phi^{(0)}_{m'-m}(q,\,l,\,0,\,0,\,2k-n+n'+3)\right], \tag{A18}$$

where

$$A_{nn'} = \sqrt{\frac{(2n'+1)}{4\pi n'(n'+1)}}\sqrt{\frac{(2n+1)}{4\pi n(n+1)}}, \tag{A19}$$

and

$$\begin{aligned} I^{(1)}_{mnm'n'}(q,\,l,\,\mu) = m&\left[\frac{n'\sqrt{(n'+1)^2-m'^2}}{2n'+1}G_{mnm'n'+1}(q,\,l,\,\mu) - \frac{(n'+1)\sqrt{n'^2-m'^2}}{2n'+1}G_{mnm'n'-1}(q,\,l,\,\mu)\right] + \\ &+m'\left[\frac{n\sqrt{(n+1)^2-m^2}}{2n+1}G_{mn+1m'n'}(q,\,l,\,\mu) - \frac{(n+1)\sqrt{n^2-m^2}}{2n+1}G_{mn-1m'n'}(q,\,l,\,\mu)\right], \end{aligned} \tag{A20}$$

$$I^{(2)}_{mnm'n'}(q,\,l,\,\mu) = |mm'|G_{mnm'n'}(q,\,l,\,\mu) + \frac{1}{(2n'+1)(2n+1)}\begin{bmatrix} (n'+1)\sqrt{n'^2-m'^2}(n+1)\sqrt{n^2-m^2}G_{mn-1m'n'-1}(q,\,l,\,\mu)+ \\ n'\sqrt{(n'+1)^2-m'^2}n\sqrt{(n+1)^2-m^2}G_{mn+1m'n'+1}(q,\,l,\,\mu)- \\ (n'+1)\sqrt{n'^2-m'^2}n\sqrt{(n+1)^2-m^2}G_{mn+1m'n'-1}(q,\,l,\,\mu)- \\ n'\sqrt{(n'+1)^2-m'^2}(n+1)\sqrt{n^2-m^2}G_{mn-1m'n'+1}(q,\,l,\,\mu) \end{bmatrix}, \tag{A21}$$

and

$$L^{(00)}_{mnm'n'}(k,\,l,\,k',\,l',\,\mu) = m'Y_{mnm'n'}(k,\,l,\,k',\,l',\,\mu), \tag{A22}$$

$$L^{(01)}_{mnm'n'}(k,\,l,\,k',\,l',\,\mu) = \frac{1}{2n'+1}\left[n'\sqrt{(n'+1)^2-m'^2}Y_{mnm'n'+1}(k,\,l,\,k',\,l',\,\mu) - (n'+1)\sqrt{n'^2-m'^2}Y_{mnm'n'-1}(k,\,l,\,k',\,l',\,\mu)\right], \tag{A23}$$

$$L^{(10)}_{mnm'n'}(k,\,l,\,\mu) = m'G_{mnm'n'}(k,\,l,\,\mu), \tag{A24}$$

$$L^{(11)}_{mnm'n'}(k,\,l,\,\mu) = \frac{1}{2n'+1}\left[n'\sqrt{(n'+1)^2-m'^2}G_{mnm'n'+1}(k,\,l,\,\mu) - (n'+1)\sqrt{n'^2-m'^2}G_{mnm'n'-1}(k,\,l,\,\mu)\right], \tag{A25}$$

and

$$\Phi^{(0)}_{m}(k,\,l,\,k',\,l',\,\mu) = \frac{1+(-1)^{m+k\mu}}{2}\sum_{p=0}^{\mu}C'^{p}_{|\mu|}(a_{lm})^p(b_{lm})^{\mu-p}\left[(a_{l'm}-ib_{l'm})\Psi_{m+k'}(k,\,p,\,\mu-p)+(a_{l'm}+ib_{l'm})\Psi_{m-k'}(k,\,p,\,\mu-p)\right], \tag{A26}$$

$$\Phi^{(1)}_{m}(k,\,l,\,k',\,l',\,\mu) = \frac{k\left[1+(-1)^{m+k\mu}\right]}{2}\sum_{p=0}^{\mu}C'^{p}_{|\mu|}(a_{lm})^p(b_{lm})^{\mu-p}\left[(b_{l'm}-ia_{l'm})\Psi_{m+k'}(k,\,p,\,\mu-p)+(b_{l'm}+ia_{l'm})\Psi_{m-k'}(k,\,p,\,\mu-p)\right], \tag{A27}$$

where $a_{l'm}$ and $b_{l'm}$ are coefficients in Eq. (3) and

$$\Psi_\tau(k,\,p,\,t) = \frac{i\pi e^{\frac{i\pi\left(\frac{\tau}{k}-p-1\right)}{2}}}{2^{p+t}k(t+1)B\left(\frac{t+p-\frac{\tau}{k}+2}{2},\,\frac{t-p+\frac{\tau}{k}}{2}+1\right)}\,{}_2F_1\left(-p,\,\frac{\frac{\tau}{k}-t-p}{2};\,\frac{t-p+\frac{\tau}{k}}{2}+1;\,-1\right), \tag{A28}$$

The function ${}_2F$(a, b; c; z) and $B(\eta,\nu)=\Gamma(\eta)\Gamma(\nu)/\Gamma(\eta+\nu)$ are the Gaussian hypergeometric and beta function, respectively, $\Gamma(\ldots)$ being the gamma function. Then

$$\begin{aligned} G_{mnm'n'}(\chi,\,l,\,\mu) = (-1)^{n+n'}&\Xi_m\Xi_{m'}n!\sqrt{(n-|m|)!(n+|m|)!}n'!\sqrt{(n'-|m'|)!(n'+|m'|)!} \\ &\times\sum_{k=0}^{n-|m|}\frac{(-1)^k}{k!(n-k)!(n-|m|-k)!(|m|+k)!}\sum_{k'=0}^{n'-|m'|}\frac{(-1)^{k'}}{k'!(n'-k')!(n'-|m'|-k')!(|m'|+k')!}F^{(1)}_{mnm'n'}(\chi,\,l,\,k,\,k',\,\mu), \end{aligned} \tag{A29}$$

$$\begin{aligned} F^{(1)}_{mnm'n'}(\chi,\,l,\,k,\,k',\,\mu) = \frac{1}{2^{l\mu}}&\sum_{p=1}^{\mu\left[\frac{l}{2}\right]}\xi_p(\mu)\sum_{q=1}^{\infty}2^q\frac{(l-2p-\chi)(l-2p-\chi+1)\ldots(l-2p-\chi+q-1)}{q!} \\ &\times\Omega\left(2n-2k-|m|+2n'-2k'-|m'|-1+2,\,2k+|m|+2k'+|m'|-1+q\right), \end{aligned} \tag{A30}$$

$$\begin{aligned}F^{(2)}_{mnm'n'}(\chi,l,\chi',l',k,k',\mu) = &-\frac{l'}{2^{l\mu+l'+2}}\sum_{p=1}^{[l/2]\mu}\xi_p(\mu)\sum_{q=1}^{\infty}2^q\frac{(l-2p-\chi)(l-2p-\chi+1)\dots(l-2p-\chi+q-1)}{q!}\\ &\times\sum_{w=0}^{[l'/2]}(-1)^w C^w_{l'}C^{l'}_{2l'-2w}\frac{\Gamma(l'-2w)}{\Gamma(l'-2w-k)}\Omega\big(2k+|m|+2k'+|m'|,2n-2k-|m|+2n'-2k'-|m'|\\ &+q+w-2\big)+\frac{l'+k'}{2^{l\mu+l'+1}}\sum_{p=1}^{[l/2]\mu}\xi_p(\mu)\sum_{q=1}^{\infty}2^q\frac{(l-2p-\chi')(l-2p-\chi'+1)\dots(l-2p-\chi'+q-1)}{q!}\\ &\times\sum_{w=0}^{[l'/2]}(-1)^w C^w_{l'-1}C^{l'-1}_{2l'-2w-2}\frac{\Gamma(l'-1-2w)}{\Gamma(l'-1-2w-k)}\\ &\times\Omega\big(2k+|m|+2k'+|m'|,\,2n-2k-|m|+2n'-2k'-|m'|+l'-1-2w-k\big),\end{aligned} \tag{A31}$$

where $[n]$ is the smallest integer greater than or equal to n. Coefficients ξ_p can be found from the following recurrence relation

$$\xi_p(\mu)=(-1)^p\mu C^p_l C^l_{2l-2p}\frac{\Gamma(l-2p)}{\Gamma(l-2p-k)}+\frac{1}{p}\sum_{q=1}^{p-1}\big[\mu(p-q)-q\big](-1)^{p-q}C^{p-q}_l C^l_{2l-2p-q}\frac{\Gamma(l-2p-2q)}{\Gamma(l-2p-2q-k)}\xi_q(\mu), \tag{A32}$$

where the initial value $\xi_0(\mu)=1$. Moreover

$$\begin{aligned}&Y_{mnm'n'}(\chi,l,\chi',l',\mu)=(-1)^{n+n'}\Xi_m\Xi_{m'}n!\sqrt{(n-|m|)!(n+|m|)!}\,n'!\sqrt{(n'-|m'|)!(n'+|m'|)!}\\ &\sum_{k=0}^{n-|m|}\frac{(-1)^k}{k!(n-k)!(n-|m|-k)!(|m|+k)!}\sum_{k'=0}^{n'-|m'|}\frac{(-1)^{k'}}{k'!(n'-k')!(n'-|m'|-k')!(|m'|+k')!}F^{(2)}_{mnm'n'}(\chi,l,\chi',l',k,k',\mu),\end{aligned} \tag{A33}$$

$$\Xi_m=\begin{cases}1, & m\ge 0\\ (-1)^m, & m<0\end{cases}, \tag{A34}$$

$$\Omega(\eta,\nu)=\frac{\Gamma\left(\frac{\eta+1}{2}\right)\Gamma\left(\frac{\nu+1}{2}\right)}{2\Gamma\left(\frac{\eta+\nu}{2}+1\right)}, \tag{A35}$$

$\delta_{n,m}=\begin{cases}1, & n=m\\ 0, & n\neq m\end{cases}$ is Kronecker's delta, and $C^m_n=\frac{n!}{m!(n-m)!}$ is the binomial coefficient.

References

[1] Mishchenko MI, Travis LD, Lacis AA. In: Scattering, absorption, and emission of light by small particles. Cambridge: Cambridge University Press; 2002 690.

[2] Petrov D, Synelnyk E, Shkuratov Y, Videen G. The *T*-matrix technique for calculations of scattering properties of ensembles of randomly oriented particles with different size. J Quant Spectrosc Radiat Transfer 2006;102:85–110.

[3] Petrov D, Shkuratov Y, Videen G. Analytical light-scattering solution for Chebyshev particles. J Opt Soc Am A 2007;24:1103–19.

[4] Petrov D, Videen G, Shkuratov Y, Kaydash M. Analytic *T*-matrix solution of light scattering from capsule and bi-sphere particles: applications to spore detection. J Quant Spectrosc Radiat Transfer 2007;108:81–105.

[5] Petrov D, Shkuratov Y, Videen G. *Sh*-matrices method applied to light scattering by finite circular cylinders. J Quant Spectrosc Radiat Transfer 2008;109:1474–95.

[6] Petrov D, Shkuratov Y, Videen G. Influence of corrugation on light-scattering properties of capsule and finite-cylinder particles: analytic solution using *Sh*-matrices. J Quant Spectrosc Radiat Transfer 2008;109:650–69.

[7] Petrov D, Shkuratov Y, Videen G. Analytic light-scattering solution of two merging spheres using *Sh*-matrices. Opt Commun. 2008;281:2411–23.

[8] Petrov D, Shkuratov Yu, Videen G. The *Sh*-matrices method as applied to scattering by microlenses. J Quant Spectrosc Radiat Transfer 2009;110:1448–59.

[9] Petrov D, Shkuratov Y, Videen G. Light scattering by a finite cylinder containing a spherical cavity using *Sh*-matrices. Opt Commun. 2009;282:156–66.

[10] Petrov D, Shkuratov Y, Videen G. An analytical solution to the light scattering from cube-like particles using *Sh*-matrices. J Quant Spectrosc Radiat Transfer 2010;111:474–82.

[11] Petrov D, Shkuratov Y, Videen G. Electromagnetic wave scattering from cuboid-like particles using *Sh*-matrices. J Quant Spectrosc Radiat Transfer 2011;112:155–62.

[12] Petrov D, Shkuratov Y, Videen G. The *Sh*-matrices method as applied to scattering by two merging spheroids. J Quant Spectrosc Radiat Transfer 2010;111:1990–9.

[13] Muinonen K. Light scattering by Gaussian random particles: Rayleigh and Rayleigh-Gans approximations. J Quant Spectrosc Radiat Transfer 1996;55:603–13.

[14] Muinonen K, Zubko E, Tyynela J, Shkuratov Y, Videen G. Light scattering by Gaussian random particles with the discrete-dipole approximation. J Quant Spectrosc Radiat Transfer 2007;106: 360–77.

[15] Abramowitz M, Stegun I. In: Handbook on Mathematical Functions. New York: National bureau of standards; 1964 832.

[16] Grynko E, Shkuratov Y. Scattering matrix calculated in geometric optics approximation for semitransparent particles faceted with various shapes. J Quant Spectrosc Radiat Transfer 2003;78(3–4): 319–40.

[17] Penttila A, Zubko E, Lumme K, Muinonen K, Yurkin M, Draine B, et al. Comparison between discrete dipole implementations and exact techniques. J Quant Spectrosc Radiat Transfer 2007;106: 417–36.

NO. OF COPIES	ORGANIZATION
1 (PDF)	ADMNSTR DEFNS TECHL INFO CTR ATTN DTIC OCP
6 (PDFS)	US ARMY RSRCH LAB ATTN IMAL HRA MAIL & RECORDS MGMT ATTN RDRL CIO LL TECHL LIB ATTN RDRL CIE S V GORDEN ATTN RDRL CIE P CLARK ATTN RDRL CIE S T DEFELICE ATTN RDRL CIE S C WILLIAMSON

INTENTIONALLY LEFT BLANK.